Expanded View Figures

Figure EV1. Generation and characterization of *Arabidopsis* NRPB2 point mutations (related to Fig 1).

A Schematic overview of a work flow to generate $NRPB2_{WT}^{+/+}$ $nrpb2\text{-}2^{-/-}$, $NRPB2_{Y732F}^{+/+}$ $nrpb2\text{-}2^{-/-}$, and $NRPB2_{P979S}^{+/+}$ $nrpb2\text{-}2^{+/-}$ *Arabidopsis*. First, constructs harboring $NRPB2_{WT}$ (blue), $NRPB2_{Y732F}$ (red), and $NRPB2_{P979S}$ (green) transgene expression cassette were transformed into wild-type (Col-0) *Arabidopsis* via *Agrobacterium*-mediated transformation; T3 transformant plants with homozygous transgenes are crossed with $nrpb2\text{-}2^{+/-}$ (gray) heterozygous *Arabidopsis*; then, plants positive for both transgenes and *nrpb2-2* allele were selected for propagation into F3 generation to screen for homozygous double mutants of transgene and *nrpb2-2*.

B Phenotype of *Arabidopsis* siliques of wild-type (Col-0), $NRPB2_{P979S}^{+/+}$ Col-0, and $NRPB2_{P979S}$ $nrpb2\text{-}2^{+/-}$ plants. Scale bars represent 10 mm.

C Silique length of wild-type (Col-0), $NRPB2_{P979S}^{+/+}$ Col-0, and $NRPB2_{P979S}^{+/+}$ $nrpb2\text{-}2^{+/-}$ plants ($n > 20$ for each genotype). Two-sided Student's *t*-test was used for statistical test, *** denotes $P < 0.001$. The solid horizontal lines and box limits represent median, lower and upper quartiles of data values in each group. The upper and lower whiskers extend to the largest or smallest value, respectively, no further than 1.5*IQR from the relevant quartile.

D Opened siliques from wild-type (Col-0), $NRPB2_{P979S}^{+/+}$ Col-0, and $NRPB2_{P979S}^{+/+}$ $nrpb2\text{-}2^{+/-}$ plants. Red arrows indicate aborted ovules.

E Phenotype of alternative transformation events to lines presented in Fig 1E. Homozygous mutant *nrpb2-2* was fully complemented by *NRPB2-FLAG* (top) and partially complemented by $NRPB2_{Y732F}$-*FLAG* (bottom). Plants were grown for 4 weeks in soil. Scale bars represent 1 cm.

F Relative expression level of *PR1*, *PR2*, and *PR5* in $NRPB2_{WT}^{+/+}$ $nrpb2\text{-}2^{-/-}$ and $NRPB2_{Y732F}^{+/+}$ $nrpb2\text{-}2^{-/-}$ by RT–qPCR. Error bars represent SEM from three independent replicates. **denotes $P < 0.01$ by two-sided Student's *t*-test.
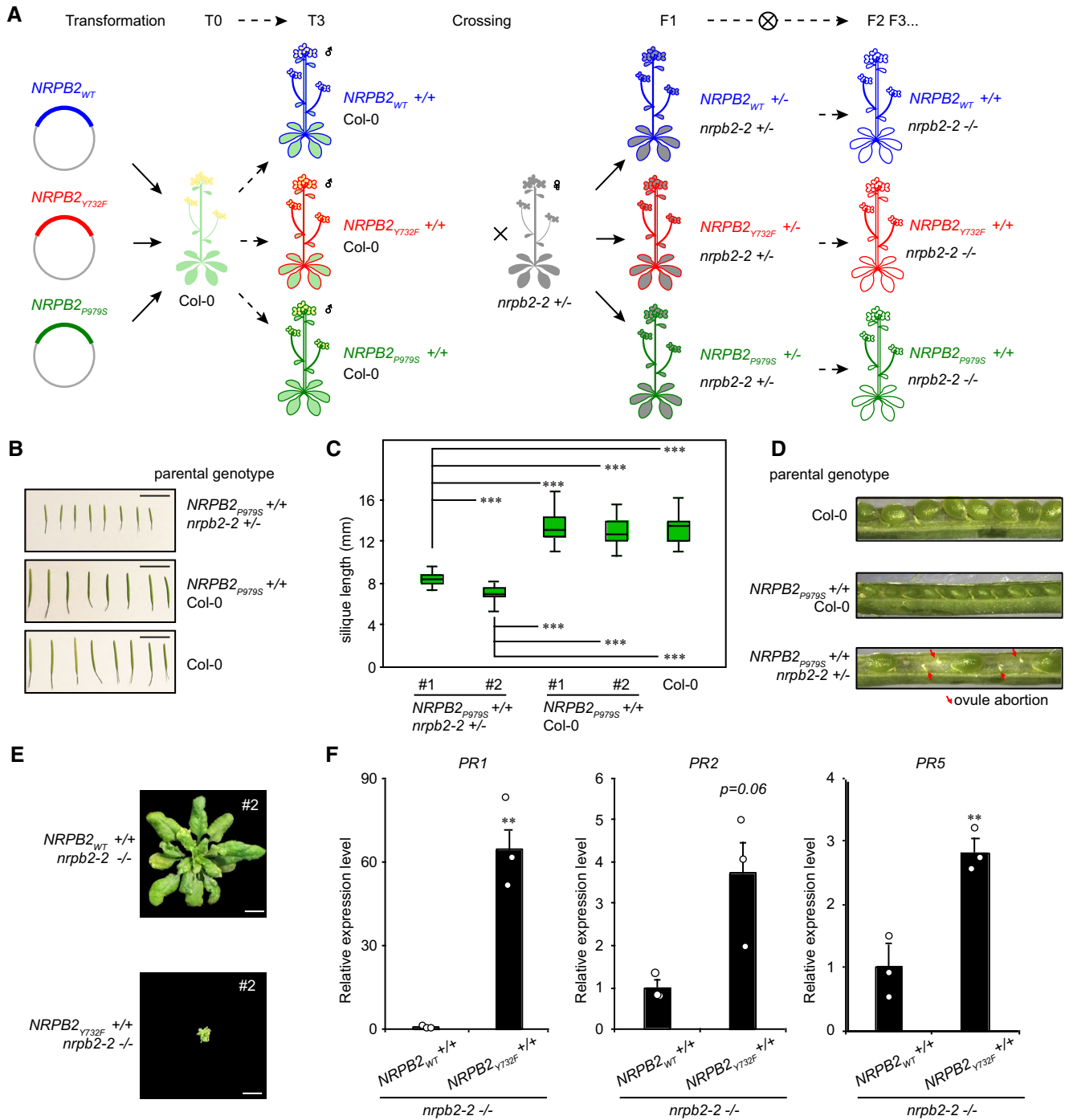
Source data are available online for this figure.

Figure EV1.

Figure EV2. Molecular and phenotypic characterization of the *rpb2-Y769F* mutation in budding yeast and *Arabidopsis* equivalent NRPB2$_{Y732F}$ (related to Fig 2).

A Differential sensitivity of various budding yeast *rpb2* mutants towards Mn^{2+} and MPA in SC-Leu media.

B Primer extension analyses for *ADH1* transcription start site usage in *rpb2* mutants in budding yeast.

C Genetic interaction between *rpb2-Y769F* and *Rpb1* TL mutations. Growth was assayed at day 1 and day 5. Ability to grow on SC-Leu + 5FOA indicates that *rpb2-Y769F* counteracts *Rpb1* TL mutations. Red box indicates the phenotype of *rpb2-Y769F* crossed with *Rpb1* TL mutations.

D A work flow of immunoprecipitation (IP) of FLAG-tagged NRPB2 protein by anti-FLAG followed by nascent RNA isolation, RT–qPCR analyses, and plaNET-seq (left). Western blotting (right) of NRPB2$_{WT}$-FLAG and NRPB2$_{Y732F}$-FLAG as IP input (input), after IP (unbound), and after elution by FLAG peptides (eluted). Upper panel shows representative anti-FLAG blots. Lower panel shows total proteins as loading control for indicated fractions.

E Nascent RNA profile of *AT5G41740*. Nascent RNA RT–qPCR assay measuring RNAPII signal at three positions (dark red bars: probes 1, 2, and 3) on gene upon flagellin 22 treatment in a 0-, 2-, 3-, and 4-min time course. Nascent RNA signal values were normalized to reference gene *ACT2*. Error bars represent SEM from 3 independent replicates. The statistical significance of differences between *NRPB2$_{Y732F}$* and *NRPB2$_{WT}$* at the same time point was assessed by two-sided Student's *t*-test. n.s. denotes not significant; * denotes $P < 0.05$; and ** denotes $P < 0.01$. Scale bar (black) represent 0.5 kb.
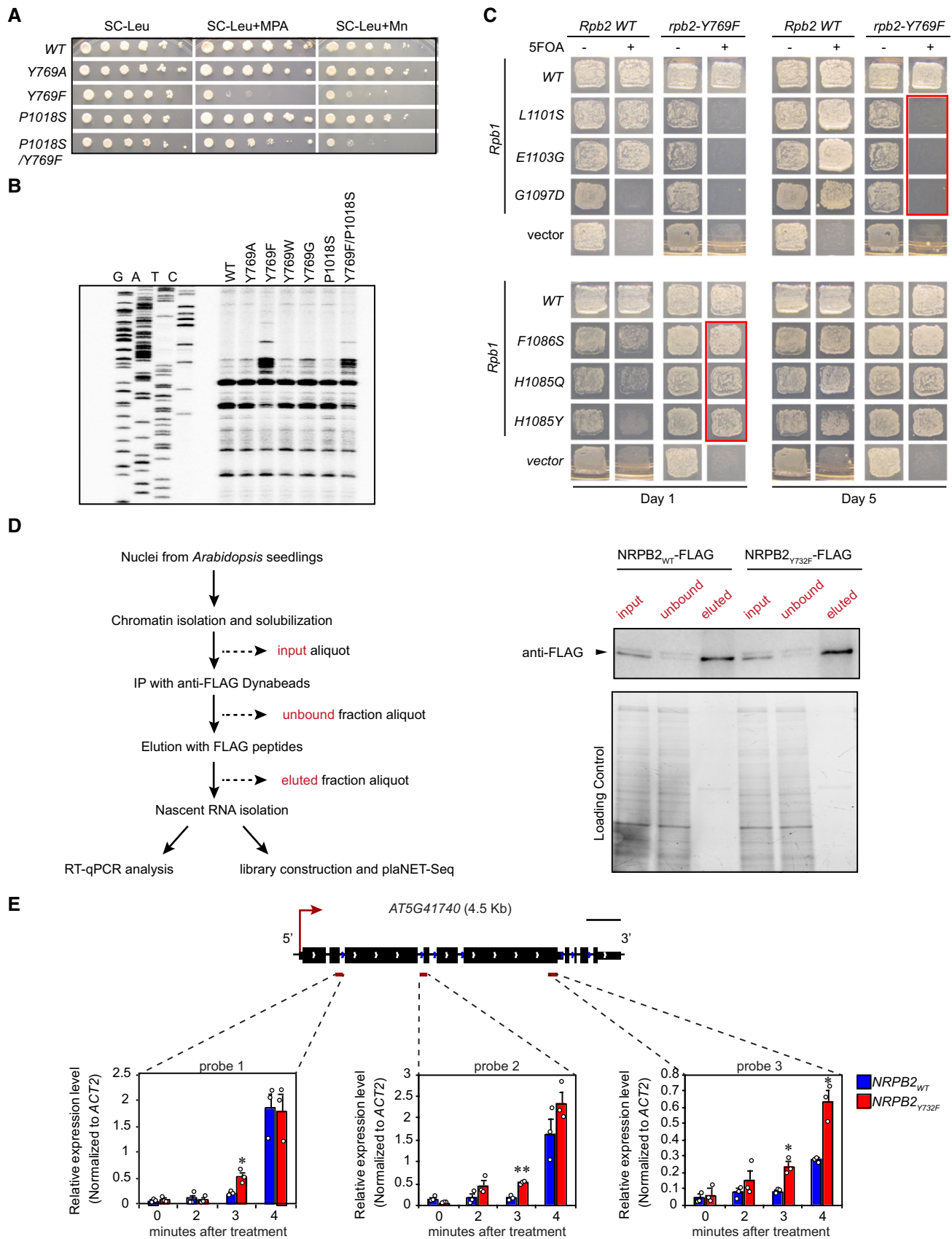
Source data are available online for this figure.

A

SC-Leu | SC-Leu+MPA | SC-Leu+Mn

WT
Y769A
Y769F
P1018S
P1018S /Y769F

B

G A T C | WT | Y769A | Y769F | Y769W | Y769G | P1018S | Y769F/P1018S

C

Rpb2 WT | *rpb2-Y769F* | *Rpb2 WT* | *rpb2-Y769F*

5FOA − + − + − + − +

Rpb1
WT
L1101S
E1103G
G1097D
vector

Rpb1
WT
F1086S
H1085Q
H1085Y
vector

Day 1 | Day 5

D

Nuclei from *Arabidopsis* seedlings

↓

Chromatin isolation and solubilization ----> input aliquot

↓

IP with anti-FLAG Dynabeads ----> unbound fraction aliquot

↓

Elution with FLAG peptides ----> eluted fraction aliquot

↓

Nascent RNA isolation

↙ ↘

RT-qPCR analysis | library construction and plaNET-Seq

NRPB2$_{WT}$-FLAG | NRPB2$_{Y732F}$-FLAG

input unbound eluted | input unbound eluted

anti-FLAG ►

Loading Control

E

AT5G41740 (4.5 Kb)

5' 3'

probe 1 | probe 2 | probe 3

Relative expression level (Normalized to *ACT2*)

minutes after treatment

■ NRPB2$_{WT}$
■ NRPB2$_{Y732F}$

Figure EV2.

Figure EV3. Genome-wide effects of $NRPB2_{Y732F}$ on nascent RNAPII transcription by plaNET-seq compared to $NRPB2_{WT}$ (related to Fig 3).

A Scatterplot showing the biological reproducibility of plaNET-seq experiment in $NRPB2_{WT}^{+/+}$ $nrpb2\text{-}2^{-/-}$. TPM-normalized plaNET-seq signal was summarized within 10-bp bins genome-wide. Pearson R = 0.987.

B Scatterplot showing the biological reproducibility of plaNET-seq experiment in $NRPB2_{Y732F}^{+/+}$ $nrpb2\text{-}2^{-/-}$. TPM-normalized plaNET-seq signal was summarized within 10-bp bins genome-wide. Pearson R = 0.987.

C Metagene profile of plaNET-seq mean signal of RNAPII in a 1 kb window centered at the TSS of *Arabidopsis* genes (n = 24,862) in $NRPB2_{WT}$ (blue) and $NRPB2_{Y732F}$ (red).

D plaNET-seq signal of RNAPII across the whole *AT2G19830* gene in $NRPB2_{WT}$ (blue) and $NRPB2_{Y732F}$ (red). Arrows indicate the elevated nascent RNAPII signal in the gene body.

E Metagene profile of plaNET-seq mean signal of RNAPII in exons (50–100 bp, scaled to 100 bins, n = 31,202) in $NRPB2_{WT}^{+/+}$ $nrpb2\text{-}2^{-/-}$ ($NRPB2_{WT}$, blue) and $NRPB2_{Y732F}^{+/+}$ $nrpb2\text{-}2^{-/-}$ ($NRPB2_{Y732F}$, red).

F Metagene profile of plaNET-seq mean signal of RNAPII in exons (100–200 bp, scaled to 100 bins, n = 33,600) in $NRPB2_{WT}^{+/+}$ $nrpb2\text{-}2^{-/-}$ ($NRPB2_{WT}$, blue) and $NRPB2_{Y732F}^{+/+}$ $nrpb2\text{-}2^{-/-}$ ($NRPB2_{Y732F}$, red).

G Metagene profile of plaNET-seq mean signal of RNAPII in exons (200–300 bp, scaled to 100 bins, n = 9,795) in $NRPB2_{WT}^{+/+}$ $nrpb2\text{-}2^{-/-}$ ($NRPB2_{WT}$, blue) and $NRPB2_{Y732F}^{+/+}$ $nrpb2\text{-}2^{-/-}$ ($NRPB2_{Y732F}$, red).

H Metagene profile of plaNET-seq mean signal of RNAPII in introns (50–100 bp, scaled to 100 bins, n = 58,050) in $NRPB2_{WT}^{+/+}$ $nrpb2\text{-}2^{-/-}$ ($NRPB2_{WT}$, blue) and $NRPB2_{Y732F}^{+/+}$ $nrpb2\text{-}2^{-/-}$ ($NRPB2_{Y732F}$, red).

I Metagene profile of plaNET-seq mean signal of RNAPII in introns (100–200 bp, scaled to 100 bins, n = 34,213) in $NRPB2_{WT}^{+/+}$ $nrpb2\text{-}2^{-/-}$ ($NRPB2_{WT}$, blue) and $NRPB2_{Y732F}^{+/+}$ $nrpb2\text{-}2^{-/-}$ ($NRPB2_{Y732F}$, red).

J Metagene profile of plaNET-seq mean signal of RNAPII in introns (200–300 bp, scaled to 100 bins, n = 128) in $NRPB2_{WT}^{+/+}$ $nrpb2\text{-}2^{-/-}$ ($NRPB2_{WT}$, blue) and $NRPB2_{Y732F}^{+/+}$ $nrpb2\text{-}2^{-/-}$ ($NRPB2_{Y732F}$, red).

K Metagene profile of plaNET-seq mean signal of RNAPII in constitutive exons (n = 75,136) in $NRPB2_{WT}^{+/+}$ $nrpb2\text{-}2^{-/-}$ ($NRPB2_{WT}$, blue) and $NRPB2_{Y732F}^{+/+}$ $nrpb2\text{-}2^{-/-}$ ($NRPB2_{Y732F}$, red).

L Metagene profile of plaNET-seq mean signal of RNAPII in alternative exons (n = 724) in $NRPB2_{WT}^{+/+}$ $nrpb2\text{-}2^{-/-}$ ($NRPB2_{WT}$, blue) and $NRPB2_{Y732F}^{+/+}$ $nrpb2\text{-}2^{-/-}$ ($NRPB2_{Y732F}$, red).

M Metagene profile of plaNET-seq mean signal of RNAPII in constitutive exons (n = 97,358) in $NRPB2_{WT}^{+/+}$ $nrpb2\text{-}2^{-/-}$ ($NRPB2_{WT}$, blue) and $NRPB2_{Y732F}^{+/+}$ $nrpb2\text{-}2^{-/-}$ ($NRPB2_{Y732F}$, red).

N Metagene profile of plaNET-seq mean signal of RNAPII in alternative exons (n = 5,306) in $NRPB2_{WT}^{+/+}$ $nrpb2\text{-}2^{-/-}$ ($NRPB2_{WT}$, blue) and $NRPB2_{Y732F}^{+/+}$ $nrpb2\text{-}2^{-/-}$ ($NRPB2_{Y732F}$, red).
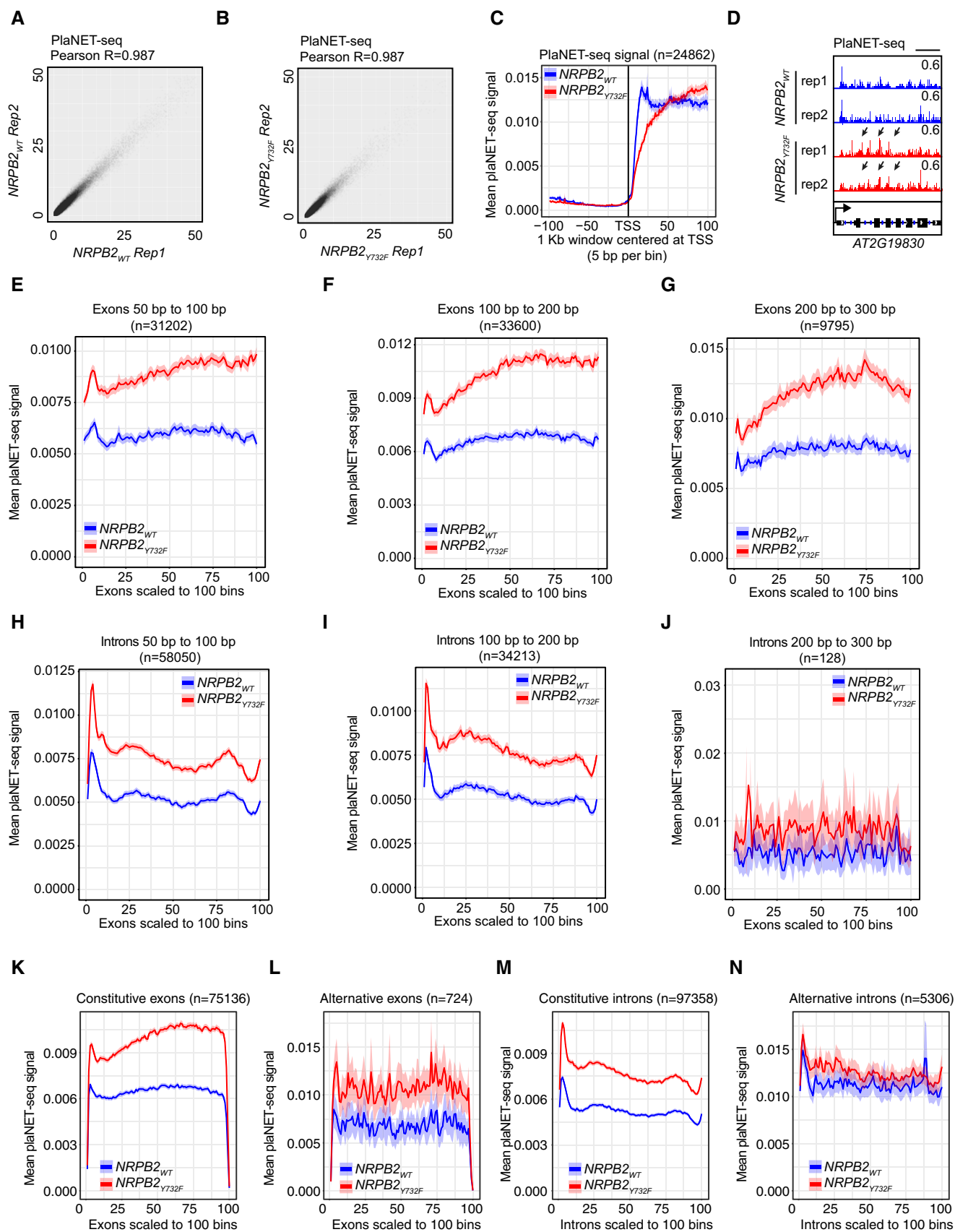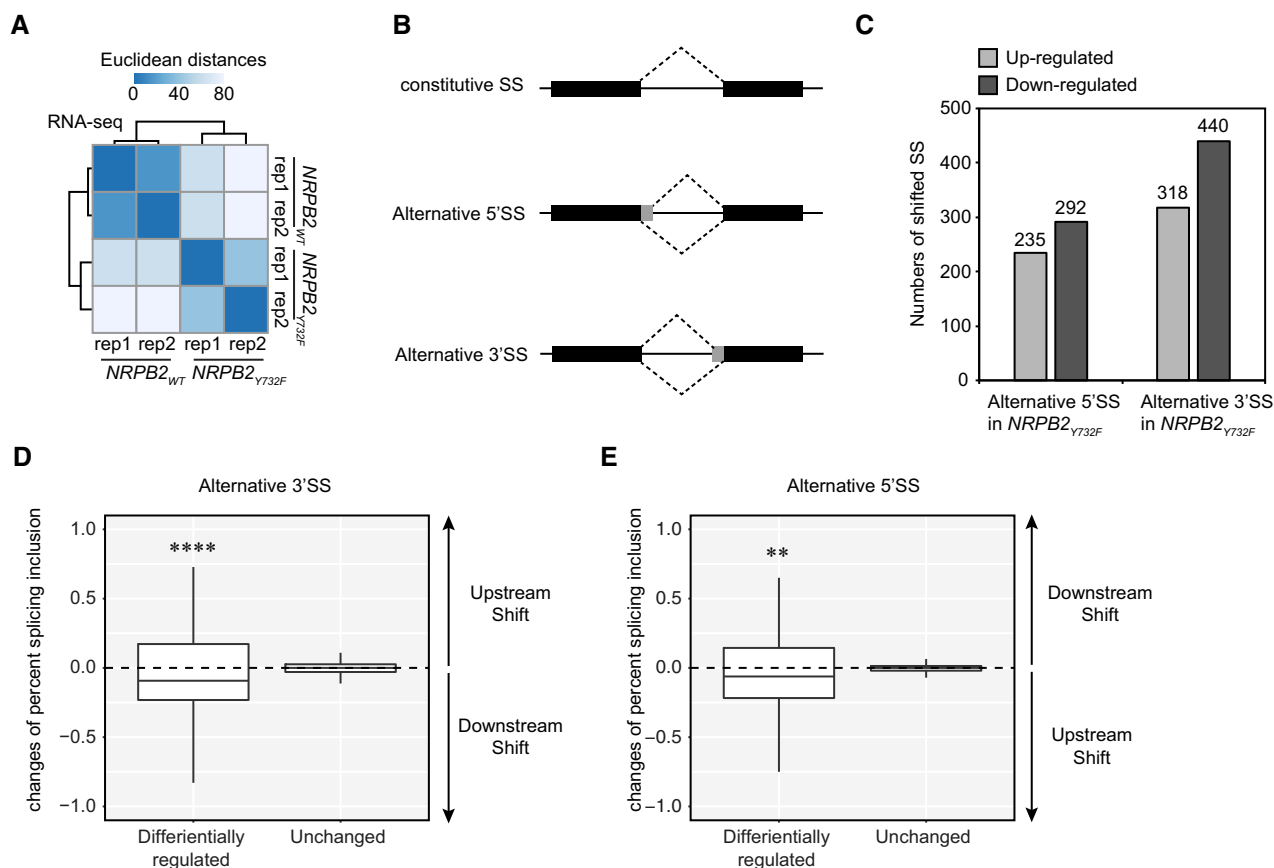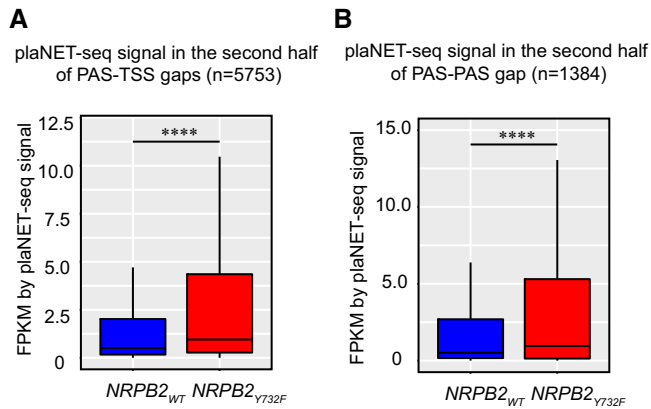
Figure EV3.

Figure EV4. Genome-wide effects of *NRPB2$_{Y732F}$* on gene expression by RNA-seq compared to *NRPB2$_{WT}$* (related to Fig 4).

A Reproducibility of RNA-seq data demonstrated by clustered heatmap of Euclidean distances between two independent replicates of RNA-seq in both *NRPB2$_{WT}$*$^{+/+}$ *nrpb2-2*$^{-/-}$ and *NRPB2$_{Y732F}$*$^{+/+}$ *nrpb2-2*$^{-/-}$. Darker blue stands for higher reproducibility, and lighter blue represents low reproducibility.

B Illustration of constitutive splicing site (SS), alternative 5′ splicing site (SS), and alternative 3′ splicing site (SS).

C Differentially regulated alternative 5′SS and 3′SS in *NRPB2$_{Y732F}$*$^{+/+}$ *nrpb2-2*$^{-/-}$ compared to *NRPB2$_{WT}$*$^{+/+}$ *nrpb2-2*$^{-/-}$ based on RNA-seq results. Numbers of up- and down-regulated SS were shown on the plot.

D Quantification (the changes of present splicing inclusion, dPSI) of differentially regulated alternative 3′SS exons and non-DE exons in *NRPB2$_{Y732F}$*$^{+/+}$ *nrpb2-2*$^{-/-}$ compared to *NRPB2$_{WT}$*$^{+/+}$ *nrpb2-2*$^{-/-}$. dPSI > 0 and dPSI < 0 suggest upstream and downstream shift of alternative 5′SS, respectively. **** denotes *P*-value < 0.0001 by Wilcoxon signed-rank test. The solid horizontal lines and box limits represent median, lower and upper quartiles of data values in each group. The upper and lower whiskers extend to the largest or smallest value, respectively, no further than 1.5*IQR from the relevant quartile.

E Quantification (the changes of present splicing inclusion, dPSI) of differentially regulated alternative 5′SS exons and non-DE exons in *NRPB2$_{Y732F}$*$^{+/+}$ *nrpb2-2*$^{-/-}$ compared to *NRPB2$_{WT}$*$^{+/+}$ *nrpb2-2*$^{-/-}$. dPSI > 0 and dPSI < 0 suggest downstream and upstream shift of alternative 5′SS, respectively. ** denotes *P*-value < 0.01 by Wilcoxon signed-rank test. The solid horizontal lines and box limits represent median, lower and upper quartiles of data values in each group. The upper and lower whiskers extend to the largest or smallest value, respectively, no further than 1.5*IQR from the relevant quartile.

A

plaNET-seq signal in the second half
of PAS-TSS gaps (n=5753)

B

plaNET-seq signal in the second half
of PAS-PAS gap (n=1384)

Figure EV5. Quantification of read-through transcription in $NRPB2_{Y732F}$ compared to $NRPB2_{WT}$ (related to Fig 5).

A Box plot showing the comparison of plaNET-seq signal of $NRPB2_{WT}$ (blue) and $NRPB2_{Y732F}$ (red) in the region corresponding to the second half of PAS-TSS gaps (n = 5,753) between tandemly oriented genes. Mann–Whitney test, **** denotes P = 1.70e-43. The solid horizontal lines and box limits represent median, lower and upper quartiles of data values in each group. The upper and lower whiskers extend to the largest or smallest value, respectively, no further than 1.5*IQR from the relevant quartile.

B Box plot showing the comparison of plaNET-seq signal of $NRPB2_{WT}$ (blue) and $NRPB2_{Y732F}$ (red) in the region corresponding to the second half of PAS-PAS gaps (n = 1,384) between genes located in "tail-to-tail" orientation. Mann–Whitney test, **** denotes P = 7.10e-14. The solid horizontal lines and box limits represent median, lower and upper quartiles of data values in each group. The upper and lower whiskers extend to the largest or smallest value, respectively, no further than 1.5*IQR from the relevant quartile.